Inflammation (2026) 49:125
https://doi.org/10.1007/s10753-025-02434-x

RESEARCH

A Novel Insight into Chronic Pancreatitis Pathogenesis: the USP1/ITGB5 Axis-Mediated Stellate Cell Activation

Dongyan Wang[1,2] · Yihai Shi[2] · Jie Lu[3] · Wen Bao[4] · Nan Wang[3] · Qiuteng Shen[1] · Zhenyu Lin[1] · Lijuan Qian[5,6] · Chang Zhu[7]

Received: 10 November 2025 / Revised: 16 December 2025 / Accepted: 18 December 2025

Abstract

Chronic pancreatitis (CP) is characterized by chronic pancreatic inflammation and progressive fibrosis. This study investigated the role of ubiquitin-specific peptidase 1 (USP1), a protein-stabilizing deubiquitinase, in CP. C57BL/6J mice were given 8-week repetitive intraperitoneal cerulein (50 μg/kg) injections to establish the CP model. USP1 expression in CP mouse pancreatic tissues was 3-fold higher than in controls. Lentivirus-mediated *Usp1* knockdown reduced pancreatic inflammatory cell infiltration, trypsin activity, and proinflammatory cytokine levels. Additionally, *Usp1* knockdown inhibits collagen deposition and fibrosis of the pancreas. In vitro, USP1 was upregulated in activated pancreatic stellate cells (PSCs) induced by TGF-β1 (5 ng/mL). *USP1* knockdown decreased the expressions of collagen type I alpha 1 chain (COL1A1), COL1A2, fibronectin, and α-smooth muscle actin (α-SMA), suppressing PSC activation and extracellular matrix production. Immunoprecipitation-liquid chromatography/mass spectrometry (IP-LC/MS) and label-free proteomics identified integrin subunit beta 5 (ITGB5) as a potential target protein of USP1. USP1 promoted ITGB5 deubiquitination/stabilization, while *USP1* knockdown reduced ITGB5 expression. Rescue experiments showed *ITGB5* overexpression reversed the inhibitory effect of *USP1* knockdown on PSC activation. Moreover, *ITGB5* knockdown inhibited PSC activation via suppressing PI3K/AKT pathway. In conclusion, *USP1* knockdown inhibits PSC activation by suppressing the ITGB5-PI3K-AKT axis, thereby alleviating the pathological progression of CP.

Keywords Chronic pancreatitis · Pancreatic stellate cell · USP1 · ITGB5 · Fibrosis

Introduction

Chronic pancreatitis (CP) is an irreversible, progressive fibrosing disorder defined by persistent chronic inflammation and acinar cell injury [1]. Patients with CP exhibit a significantly elevated risk of pancreatic tumor development [2]. However, effective therapeutic interventions for this condition remain scarce. Activated pancreatic stellate cells (PSCs) proliferate, migrate to sites of tissue damage, and synthesize extracellular matrix (ECM) components—processes

Dongyan Wang and Yihai Shi contributed equally to this work.

✉ Chang Zhu
3322141@zju.edu.cn

1 School of Gongli Hospital Medical Technology, University of Shanghai for Science and Technology, Shanghai 200093, China

2 Department of Gastroenterology, Gongli Hospital of Shanghai Pudong New Area, 219 Miao Pu Road, Shanghai 200135, China

3 Department of Gastroenterology, First People's Hospital Affiliated to School of Medicine, Shanghai Jiaotong University, 85 Wujin Road, Shanghai 200080, China

4 Clinical Research Unit, Institute of Clinical Science, Zhongshan Hospital of Fudan University, Shanghai 200032, China

5 Postgraduate training base at Shanghai Gongli Hospital, Ningxia medical university, Shanghai 200135, China

6 Department of Infectious Diseases, Gongli Hospital of Shanghai Pudong New Area, 219 Miao Pu Road, Shanghai 200135, China

7 Department of Gastroenterology, Sir Run Run Shaw Hospital, College of Medicine, Zhejiang University, No.3 Qingchun East Road, Shangcheng District, 310016 Hangzhou City, Zhejiang Province, China

Published online: 19 March 2026

that initially support pancreatic tissue repair. Nevertheless, sustained PSC activation is recognized as a central driver in the pathogenesis of CP and the progression of pancreatic fibrosis [3]. Given this critical role, targeting and inhibiting the excessive activation of PSCs has emerged as a promising therapeutic strategy for CP.

The ubiquitin-proteasome system is a core component of the ubiquitin-proteasome pathway, playing a pivotal role in regulating diverse biological processes, including cell proliferation and differentiation [4, 5]. Ubiquitin-Specific Peptidase 1 (USP1), a member of the USP family of deubiquitinases, modulates cellular biological functions by removing ubiquitin moieties from target proteins [6]. Previous studies have demonstrated that USP1 promotes apoptosis and dedifferentiation of pancreatic β-cells in the context of diabetes; conversely, USP1 inhibition alleviates diabetes-induced β-cell loss [7, 8]. USP1 has been shown to facilitate the progression of pancreatic ductal adenocarcinoma [9]. Furthermore, USP1 disrupts K48-linked ubiquitination of nucleotide-binding oligomerization domain-like receptor pyrin domain-containing 3 (NLRP3), thereby inhibiting NLRP3 degradation, promoting NLRP3 inflammasome activation, and enhancing the production of inflammatory factors [10]. More importantly, USP1 activates hepatic stellate cells and promotes liver fibrosis by inhibiting SNAIL ubiquitination and stabilizing its protein expression [11]. Despite these well-characterized roles in other pathological contexts, the functional role of USP1 in CP remains largely undefined.

Integrin subunit beta 5 (ITGB5), also known as Integrin β5, participates in cell adhesion and cell surface-mediated signaling. ITGB5 encodes a subunit of integrin that interacts with multiple α-chains to form a diverse array of integrin heterodimers. The cytoplasmic tails of ITGB5 contains four lysines and can be ubiquitinated [12]. Specifically, reducing ITGB5 ubiquitination levels decreases the degradation rate of internalized β5 and promotes its accumulation on the cell surface [13]. Inhibiting integrin degradation favors the recirculation of ECM-bound integrins at the cell surface, which disrupts normal cell adhesion function and drives pathological cell adhesion and ECM deposition [14]. Notably, *USP10* overexpression suppresses ITGB5 ubiquitination and increases its protein levels, which in turn upregulates the expression of fibrosis markers α-smooth muscle actin (α-SMA) and fibronectin (FN) [15]. Conversely, integrin inhibition abrogates USP10-induced expression of α-SMA and fibronectin extra domain A (FN-EDA) [15]. Hence, these findings suggest that targeting deubiquitinase activity may represent a novel strategy to modulate cell surface integrin expression and mitigate the development of integrin-related pathological conditions.

This study aimed to investigate the role of USP1 in PSC activation and pancreatic fibrosis during CP. Using proteomics analysis, ITGB5 was identified as a potential downstream target of USP1. On this basis, the role of the USP1-ITGB5 axis in the activation of human PSCs and the pathological development of pancreatic fibrosis in CP was further explored.

Methods

GSE41418 Analysis

The GSE41418 dataset is obtained from National Center for Biotechnology Information (NCBI) Gene Expression Omnibus database (http://www.ncbi.nlm.nih.gov/geo/). Differentially expressed genes (DEGs) in pancreatic tissues of cerulein treated mice and control mice were analyzed. The DEGs in GSE41418 dataset were filtered according to $|\log2FC| > 2$ and adjust $P < 0.05$.

Animal Model

Eight-week-old C57BL/6J mice were used for establishment CP model. Mice were intraperitoneally injected with 50 μg/kg cerulein (B803321, Macklin, Shanghai, China) six time per day at 1 h intervals, 3 times per week, injection for 1, 2, 4, or 8 weeks [16]. Control mice received an equal volume of saline. To avoid the acute reaction period, two days after the last injection, mice were sacrificed and pancreatic tissues were collected. Subsequent assessment was conducted after week cerulein induction. The study was approved by the ethics committee of Sir Run Run Shaw Hospital (SRRSH202402287).

Lentivirus Construction

Lentiviral vectors were purchased from Hunan Fenghui Biotechnology Co., Ltd. (Changsha, China), including shRNA vectors (BR004) and the overexpression vector pLVX-IRES-puro (BR025). The mice were intraperitoneally injected with 2×10^6 TU of the lentivirus [17], and CP was induced 2 weeks later. The target sequences of shRNA vectors were as follows: Lv-Mus-*Usp1*-shRNA: 5'-AGAG AAATATACAGATGAACT-3'; Lv-Homo-*USP1*-shRNA: 5'-GGATTGTAGGAGAAGATAAAT-3'; Lv-Homo-*ITGB5*-shRNA: 5'-CTGAGGGCAAACCTTGTCAAA-3'; and negative control (Lv-NC): 5'-TTCTCCGAACGTG TCACGT-3'. The homo sapiens *ITGB5* gene was cloned into the multiple cloning sites (MCS) of pLVX-IRES-puro digested with XhoI and BamHI. Lentiviruses were produced using HEK293T cells.

Histopathological Analysis

Pancreatic tissues were fixed with 4% paraformaldehyde for histological examination. Fixed tissues underwent graded ethanol (10009218, SINOPHARM, Shanghai, China) dehydration, xylene (1330-20-7, Aladdin, Shanghai, China) clearing, and paraffin embedding. Following paraffin block formation, 5 μm sections were cut, dewaxed, and rehydrated. For hematoxylin-eosin (H&E) staining, sections were stained with hematoxylin solution (H8070, Solarbio, Beijing, China) for 5 min, differentiated in 1% hydrochloric acid-alcohol for 3 s, and counterstained with eosin solution (A600190, Sangon, Shanghai, China) for 3 min. Subsequent to ethanol dehydration and xylene clearing, sections were mounted with neutral balsam. Images were captured under a light microscope (BX53, Olympus, Tokyo, Japan), and pathological scoring was performed in accordance with previously established criteria [16]. Inflammatory cell infiltration: 0 (absent), 1 (< 5%), 2 (5–10%), 3 (10–50%), and 4 (≥ 50%); acinar atrophy: 0 (absent), 1 (minimal), 2 (moderate), and 3 (major/severe); fibrosis: 0 (absent), 2 (focal distribution), and 4 (diffuse distribution). The total pathological score was calculated as the sum of individual parameter scores.

For Sirius red staining, deparaffinized and rehydrated sections were stained with Sirius red solution (G1471, Solarbio, Beijing, China) mixed with picric acid for 5 min. Following ethanol dehydration and xylene clearing, sections were mounted with neutral balsam and visualized under a light microscope (BX53, Olympus, Tokyo, Japan), with images captured accordingly.

Trypsin Activity Detection

Trypsin activity was detected using a trypsin activity colorimetric assay kit (E-BC-K843-M, Elabscience, Wuhan, China). Briefly, pancreatic tissues were homogenized in reagent I and supernatants were collected by centrifugation at 10,000×g for 10 min at 4 °C. Reaction working solution and standard solution were prepared strictly following the manufacturer's instructions. Subsequently, 10 μL of sample was added to each microplate well, followed by 160 μL of reaction working solution. After incubation at 37 °C for 10 min, the absorbance at 405 nm was measured using a microplate reader (ELX-800, BIOTEK, Burlington, Vermont, USA).

Hydroxyproline Detection

Hydroxyproline content in pancreatic tissues was determined using a Hydroxyproline Assay Kit (A030, Nanjing Jiancheng Bioengineering Institute, China), following the manufacturer's instructions.

Cell Culture

Primary human pancreatic stellate cells (hPSCs) were purchased from Cellverse Biotechnology (Shanghai, China). Cells were cultured at 37 °C in a humidified incubator with 5% CO_2. For human TGF-β1 (hTGF-β1) induction, cells were treated with 5 ng/mL hTGF-β1 (HY-P78668, MCE, New Jersey, USA) for 0, 12, 24, or 48 h. For lentiviral infection, cells were cultured in virus-containing medium for 48 h; subsequently, infected cells were treated with 5 ng/mL hTGF-β1 for 24 h for further analysis. The PI3K agonist 740 YP (Y413859) was purchased from Aladdin (Shanghai, China). For 740 YP treatment, cells were pretreated with 20 μM 740 YP for 2 h, followed by hTGF-β1 stimulation for an additional 24 h.

Enzyme-linked Immunosorbent Assay (ELISA)

ELISA was performed following the manufacturers' instructions using the respective kits. Mouse Tumor Necrosis Factor-α (TNF-α) ELISA Kit (EK282), Mouse Interleukin-6 (IL-6) ELISA Kit (EK206), Mouse Interleukin-1β (IL-1β) ELISA Kit (EK201B), and Mouse TGF-β1 ELISA Kit (EK981) were purchased from Lianke Biotechnology CO., Ltd. (Hangzhou, China). Mouse Platelet-Derived Growth Factor Subunit B (PDGFB) ELISA Kit (EM0269) was purchased from Wuhan Fine Biological Technology Co., Ltd (Wuhan, China).

Real time PCR

Total RNA was extracted from pancreatic tissues using TRIpure reagent (RP1001, BioTeke, Beijing, China) according to the manufacturer's instructions. RNA concentration of each sample was measured with a Nanodrop One spectrophotometer (Thermo Fisher Scientific, Waltham, USA). Complementary DNA (cDNA) was synthesized using the All-in-One First-Strand SuperMix (MD80101, Magen Biotechnology, Guangzhou, China). Quantitative real-time PCR for gene expression analysis was performed on an ExicyclerTM 96 system (Bioneer, Daejeon, Korea), using 2×Taq PCR MasterMix (PC1150, Solarbio, Beijing, China) and SYBR Green reagent (SR4110, Solarbio, Beijing, China). Primer sequences are listed in Table 1.

Western Blot (WB)

Total proteins were extracted from pancreatic tissues and hPSCs using RIPA protein lysis buffer (PR20001, Proteintech, Wuhan, China). Protein concentration of each sample was determined using a BCA assay kit (PK10026, Proteintech, Wuhan, China). Extracted proteins were separated by

Table 1 Primer sequences.

Gene name	Primer sequences (5'-3')
mus *Usp1* F	TGAGGAATACGGAGGACG
mus *Usp1* R	CTTCTGTGAGGGCTTTGC
homo *USP1* F	TATTTGCGGTTGTGATG
homo *USP1* R	GTCCTCCAAGAAGTCCA

Table 2 The detailed information for antibodies used in this study.

Antibody	Catalog	Dilution ratio	Vendor	Application
Primary antibody				
USP1	14346-1-AP	1: 1000	Proteintech	WB/IP
FN	A16678	1: 1000	ABclonal	WB
COL1A1	R26615	1: 500	Zenbio	WB
COL1A2	343,277	1: 500	Zenbio	WB
ITGB5	SC398214	1:1000	Santa Cruz	WB/IP
PI3K	AF6242	1:1000	Affinity	WB
p-PI3K	AF3242	1:1000	Affinity	WB
AKT	AF6261	1:1000	Affinity	WB
p-AKT	AF0016	1:1000	Affinity	WB
β-actin	66009-1-Ig	1: 20,000	Proteintech	WB
α-SMA	AF1032	1: 100	Affinity	IF
COL1A1	AF7001	1: 100	Affinity	IF
Ubiquitin	Ab134953	1:3000	Abcam	IP
Secondary antibody				
Goat anti-rabbit IgG-HRP	SA00001-2	1: 10,000/1:5000	Proteintech	WB/IP
Goat anti-mouse IgG-HRP	SA00001-1	1: 10,000	Proteintech	WB
Goat anti-rabbit IgG-Alexa Fluor	A27039	1: 200	Invitrogen	IF

sodium dodecyl sulfate–polyacrylamide gel electrophoresis (SDS–PAGE) (PR20003, Proteintech, Wuhan, China) and then transferred onto polyvinylidene fluoride (PVDF) membranes (LC2005, Thermo Fisher Scientific, Waltham, USA). Then the membranes were incubated with primary antibodies at 4 °C overnight followed by incubation with secondary antibodies. Protein bands were visualized using an enhanced chemiluminescence detection kit (PK10003, Proteintech, Wuhan, China) and quantified with Gel-Pro-Analyzer. Detailed information for the antibodies is listed in Table 2.

Immunofluorescence

Paraffin-embedded tissues were sectioned into 5 μm slices. Sections were deparaffinized with xylene and rehydrated with ethanol, followed by antigen retrieval. Thereafter, sections were blocked with 1% bovine serum albumin (BSA; A602440-0050, Sangon Biotech, Shanghai, China) for 15 min. Sections were incubated with primary antibodies at 4 °C overnight, then with secondary antibodies for 60 min. Cell nuclei were stained with dihydrochloride (DAPI, D106471-5 mg, Aladdin, Shanghai, China). Stained sections were observed and imaged using a microscope (BX53, Olympus, Tokyo, Japan).

Cell slides were fixed with 4% paraformaldehyde, then permeabilized with 0.1% Triton X-100 (ST795, Beyotime, Shanghai, China) and blocked with 1% BSA (A602440-0050, Sangon Biotech, Shanghai, China). Slides were incubated with primary antibodies, followed by incubation with secondary antibodies. Cell nuclei were stained with DAPI (D106471-5 mg, Aladdin, Shanghai, China). Images were captured using a microscope (BX53, Olympus, Tokyo, Japan). Detailed information for all antibodies used is listed in Table 2.

Co-immunoprecipitation (Co-IP) and Ubiquitination Assay

Proteins were extracted using RIPA protein lysis buffer (PR20001, Proteintech, Wuhan, China) and protein concentration was measured using BCA kit (PK10026, Proteintech, Wuhan, China). The extracted proteins were mixed with specific antibodies or IgG (as a negative control), and incubated with incubation buffer at 4 °C overnight. Subsequently, the protein-antibody complexes were incubated with 80 μL Protein G beads (PR40025, Proteintech, Wuhan, China) for 2 h at 4 °C. Finally, the immunoprecipitated proteins were collected and subjected to western blot analysis and ubiquitination detection.

Immunoprecipitation-Liquid Chromatography/Mass Spectrometry (IP-LC/MS)

To identify downstream targets of USP1, the immunoprecipitated products of USP1 (derived from hPSCs and hTGF-β1-treated hPSCs) were separated using high-performance liquid chromatography (HPLC; RIGOL L-3000, RIGOL TECHNOLOGIES Co., Ltd., Beijing, China). Mass spectrometric data were analyzed with Proteome Discoverer software (Version 2.4) against the Homo sapiens UniProt database.

Label Free Proteomic

The hPSCs subjected to TGF-β treatment and *USP1* knockdown were sent to Beijing Qinglian Biotech Co., Ltd. for proteomics analysis. Briefly, proteins were extracted first and incubated with 5 mM dithiothreitol (DTT; M109-5G, Amresco, Solon, USA) at 37 °C for 1 h, followed by

incubation with 10 mM iodoacetamide at room temperature for 45 min in the dark. Proteins were then digested with trypsin at a trypsin-to-protein ratio of 1:50 overnight at 37 °C, and formic acid was added to adjust the pH. Peptides were desalted using a C18 desalting column; the desalted samples were collected and freeze-dried. Freeze-dried samples were dissolved in 0.1% formic acid solution, centrifuged at 14,000×g for 20 min, and the supernatants were collected. Subsequently, peptides were fractionated using a RIGOL L-3000 HPLC system (RIGOL TECHNOLOGIES Co., Ltd., Beijing, China) and then analyzed with a Q Exactive HF-X mass spectrometer (Thermo Fisher Scientific, Waltham, USA). Raw data were analyzed using Proteome Discoverer software (Version 2.4) against the homo sapiens UniProt database.

Data Analysis

All data were first tested for normality and homogeneity of variance. Multiple group comparisons were analyzed using one-way analysis of variance (ANOVA), followed by Tukey's multiple comparisons test. A value of $P<0.05$ was considered statistically significant. All statistical analyses were performed using GraphPad Prism 9.0 software, and data are presented as the mean ± standard deviation (SD).

Results

USP1 Is Upregulated in Pancreatic Tissues of cerulein-induced Mice

In the GSE41418 dataset, a heatmap illustrates the DEGs in pancreatic tissues of cerulein-induced CP mice (Fig. 1A). Subsequent Gene Ontology (GO) enrichment analysis of these DEGs revealed significant enrichment in biological processes associated with inflammation, fibrosis, and ubiquitination (Fig. 1B). Among these processes, genes related to deubiquitination were notably upregulated (Figs. 1C-D), and Gene Set Enrichment Analysis (GSEA) further confirmed the involvement of ubiquitination in CP pathogenesis (Fig. 1E). Given its more prominent upregulation, *Usp1* was selected for subsequent investigations. A mouse model of CP was established via cerulein administration. Pathological analysis of cerulein-induced pancreatic tissues showed inflammatory infiltration, fibrosis, and acinar atrophy, with pancreatic injury exacerbating as the cerulein injection duration increased (Fig. 1F). One week after cerulein induction, the pancreas-to-body weight ratio was decreased (Fig. 1G). Additionally, Sirius Red staining demonstrated extensive collagen deposition and fibrosis in pancreatic tissues at 2 weeks post-induction (Fig. 1H). Consistent with the GSE41418 dataset findings, USP1 expression was upregulated following cerulein induction (Fig. 1I). The experimental protocol for establishing the CP mouse model is outlined in Fig. 1J. Based on these collective results, mice subjected to 8 weeks of cerulein induction were selected for subsequent experiments.

Usp1 Knockdown Alleviates the Progression of CP Induced by Cerulein in Mice

Lentiviral-mediated *Usp1* knockdown was performed in mice (Fig. 2A-B). H&E staining demonstrated that USP1 silencing effectively alleviated cerulein-induced pathological lesions in the pancreas of CP mice, including inflammatory cell infiltration, acinar atrophy, and fibrosis (Fig. 2C-G). Consistent with these histological improvements, the pancreas-to-body weight ratio revealed that *Usp1* knockdown mitigated pancreatic atrophy in CP mice (Fig. 2H). Furthermore, *Usp1* knockdown significantly inhibited the cerulein-induced elevation of trypsin activity in pancreatic tissues (Fig. 2I). Collectively, these findings indicate that *Usp1* knockdown alleviates cerulein-induced pancreatic injury in mice.

Usp1 Knockdown Diminishes Pancreatic Inflammation and Fibrosis

Progressive inflammation is a hallmark of CP, and we therefore detected inflammatory factors in pancreatic tissues. As shown in Fig. 3A, the expression levels of TNF-α, IL-1β, and IL-6 were upregulated in the pancreatic tissues of CP mice. Notably, this upregulation was reversed by *Usp1* knockdown. Sirius Red staining further revealed that *Usp1* knockdown led to a marked reduction in collagen deposition and fibrosis in the pancreatic tissues (Fig. 3B). Consistent with this observation, *Usp1* knockdown decreased the hydroxyproline content, a signature amino acid of collagen, in pancreatic tissues (Fig. 3C), which further confirms that *Usp1* knockdown alleviates collagen deposition in the pancreas. TGFB1 and PDGFB are key mediators of PSC activation, and their expression was found to be upregulated in CP. *Usp1* knockdown resulted in a significant downregulation of TGFB1 and PDGFB expression (Fig. 3D-E). Additionally, *Usp1* knockdown effectively reduced α-SMA expression (Fig. 3F), further confirming its inhibition of PSC activation. These data suggest that *Usp1* knockdown exerts a suppressive effect on pancreatic inflammation and fibrosis.

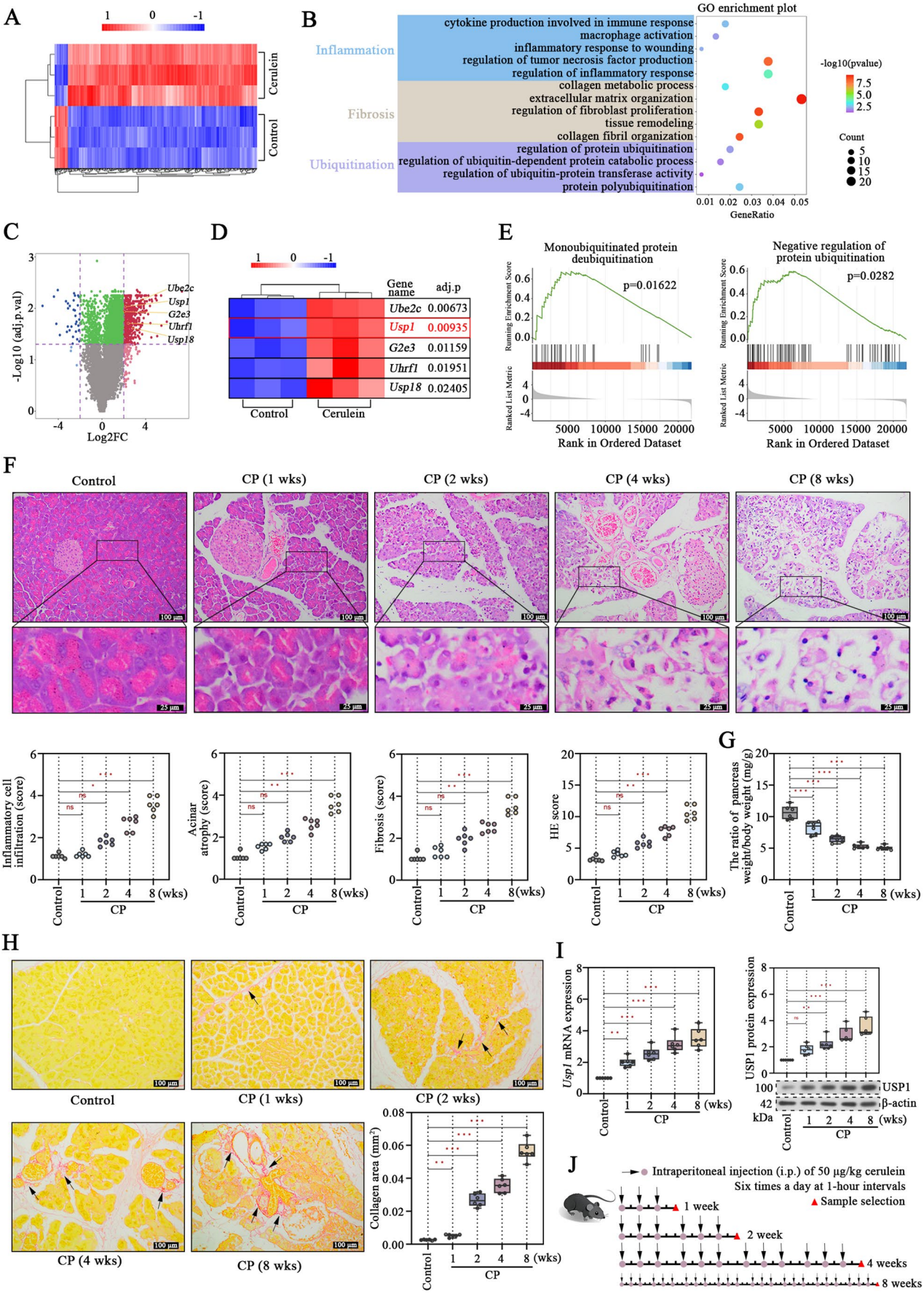
A
1 0 -1
Cerulein
Control
B
GO enrichment plot
Inflammation
Fibrosis
Ubiquitination
cytokine production involved in immune response
macrophage activation
inflammatory response to wounding
regulation of tumor necrosis factor production
regulation of inflammatory response
collagen metabolic process
extracellular matrix organization
regulation of fibroblast proliferation
tissue remodeling
collagen fibril organization
regulation of protein ubiquitination
regulation of ubiquitin-dependent protein catabolic process
regulation of ubiquitin-protein transferase activity
protein polyubiquitination
0.01 0.02 0.03 0.04 0.05
GeneRatio
-log10(pvalue)
7.5
5.0
2.5
Count
5
10
15
20
C
-Log10 (adj.p.val)
Log2FC
Ube2c
Usp1
G2e3
Uhrf1
Usp18
D
1 0 -1
Gene name
adj.p
Ube2c 0.00673
Usp1 0.00935
G2e3 0.01159
Uhrf1 0.01951
Usp18 0.02405
Control
Cerulein
E
Monoubiquitinated protein deubiquitination
p=0.01622
Negative regulation of protein ubiquitination
p=0.0282
Running Enrichment Score
Ranked List Metric
Rank in Ordered Dataset
F
Control
CP (1 wks)
CP (2 wks)
CP (4 wks)
CP (8 wks)
100 μm
25 μm
Inflammatory cell infiltration (score)
Acinar atrophy (score)
Fibrosis (score)
HE score
ns
Control
1 2 4 8 (wks)
CP
G
The ratio of pancreas weight/body weight (mg/g)
H
Control
CP (1 wks)
CP (2 wks)
CP (4 wks)
CP (8 wks)
Collagen area (mm²)
I
Usp1 mRNA expression
USP1 protein expression
USP1
β-actin
kDa
100
42
J
Intraperitoneal injection (i.p.) of 50 μg/kg cerulein
Six times a day at 1-hour intervals
Sample selection
1 week
2 week
4 weeks
8 weeks

Fig. 1 USP1 is upregulated in cerulein-induced pancreatic tissues. (**A**) Heat map of differentially expressed genes (DEGs) in GSE41418 ($n=3$) (|Log2FC|>2 and adj P value<0.05). (**B**) GO enrichment analysis of DEGs in GSE41418. (**C**) Volcano plot shows DEGs in GSE41418. **D** Heat map of ubiquitin-related genes in GSE41418. **E**. Gene sets enrichment analysis (GSEA) of deubiquitination-related terms. **F**. H&E staining and pathological score ($n=6$). Bar: up, 100 μm; down, 25 μm. **G**. The ratio of pancreas weigh/body weight ($n=6$). **H**. Sirius red staining of mouse pancreatic tissues (n=6). Bar: 100 μm. Black arrows indicate areas of fiber deposition. **I**. USP1 expression in pancreatic tissues of cerulein-induced mice was detected by real-time PCR and western blot (n=6). **J**. Flow chart for establishing a mouse model of CP. ns: not significant; *, $p<0.05$; **, $p<0.01$; ***, $p<0.001$

USP1 Knockdown Inhibits the Activation of PSCs and Decreased ECM

USP1 expression in hTGF-β1-treated PSCs was significantly increased in a time-dependent fashion (Fig. 4A-B). The knockdown efficiency of the lentiviral vector used was verified and presented in Fig. 4C-D. A heatmap illustrates the differentially expressed proteins (DEPs) identified via proteomic analysis in PSCs with *USP1* knockdown (Fig. 4E). GO enrichment analysis revealed that the DEPs are primarily involved in the collagen biosynthetic process, fibroblast growth factor signaling, and cell-matrix adhesion (Fig. 4F). Notably, collagen proteins were downregulated in *USP1*-knockdown PSCs (Fig. 4G). Consistent with this finding, *USP1* knockdown abrogated the hTGF-β1-induced upregulation of COL1A1, COL1A2, and FN protein levels in PSCs (Fig. 4H). Furthermore, *USP1* knockdown reduced the fluorescence intensity of COL1A1 and α-SMA in hTGF-β1-stimulated PSCs (Fig. 4I-K). Collectively, these results further demonstrate that *USP1* knockdown suppresses ECM accumulation and inhibits PSC activation.

ITGB5 Is the Downstream Target of USP1

IgG was used to exclude non-specific protein binding. Screening of proteins specifically interacting with USP1 in TGF-β1-stimulated PSCs identified 2015 targets (Fig. 5A). GO enrichment and Kyoto Encyclopedia of Genes and Genomes (KEGG) pathway analyses showed these proteins were linked to collagen biosynthesis and ubiquitination (Fig. 5B). Cross-analysis of USP1-specific binding proteins, significantly downregulated proteins identified in proteomics, and significantly upregulated genes from the GSE41418 dataset revealed ITGB5 as the sole common target (Fig. 5C). The String database was used to analyze the protein-protein interaction (PPI) network of DEPs, with Fig. 5D showing ITGB5-associated DEPs. Verification of ITGB5 expression in TGF-β1-treated PSCs and CP mice demonstrated its upregulation in both models, which was reversed by *USP1* knockdown (Fig. 5E-F). A Co-IP assay confirmed the interaction between USP1 and ITGB5 (Fig. 5G). Furthermore, ubiquitination assays revealed that knockdown of *USP1* promoted the ubiquitination of ITGB5, thereby facilitating its protein degradation (Fig. 5H). Collectively, these findings indicate that USP1 enhances the expression of ITGB5 through deubiquitinating it.

ITGB5 Knockdown Inhibits the PI3K/AKT Pathway To Inhibit PSC Activation

Lentivirus-mediated knockdown of *ITGB5* (Fig. 6A) reduced the protein levels of COL1A1 and FN in TGF-β1-induced PSCs (Fig. 6B-C). *ITGB5* silencing also decreased PSC activation, as evidenced by reduced α-SMA expression (Fig. 6D). Among the top 10 KEGG pathways enriched by DEPs in proteomics (Fig. 6E), the PI3K/AKT signaling pathway is known to be involved in PSC activation. Our results showed that TGF-β1 treatment activated the PI3K/AKT pathway, while *ITGB5* knockdown reduced PI3K and AKT phosphorylation (Fig. 6F-G). To further investigate the role of the PI3K/AKT pathway in PSC activation, PSCs were treated with the PI3K agonist 740 YP. Activation of the PI3K/AKT pathway upregulated COL1A1, FN, and α-SMA expression in PSCs with *ITGB5* knockdown (Fig. 6H-J), demonstrating that *ITGB5* knockdown inhibits PSC activation by suppressing the PI3K/AKT pathway.

USP1 Promotes Fibrosis in PSCs by Regulating ITGB5 Expression

A lentiviral vector was used to achieve *USP1* knockdown and *ITGB5* overexpression in PSCs (Fig. 7A). *ITGB5* overexpression reversed the inhibitory effect of USP1 knockdown on COL1A1 and FN protein expression (Fig. 7B-C). Immunofluorescence results showed that *ITGB5* overexpression increased α-SMA expression in *USP1*-knockdown PSCs (Fig. 7D). These findings indicate that *USP1* knockdown alleviates PSC activation and collagen fibril formation by suppressing ITGB5 expression.

Discussion

CP is a chronic progressive disease characterized by pancreatic inflammation and irreversible fibrosis, which ultimately leads to the gradual loss of pancreatic function [18]. Cerulein, an ortholog of cholecystokinin, promotes the activation of digestive enzymes, thereby inducing acinar cell damage and an inflammatory response that mimics pancreatitis [19–21]. Notably, repeated cerulein injections induce pancreatitis and fibrosis in mice, with pathological features similar to those of human CP [22]. Therefore, cerulein has been widely used to investigate the pathogenesis of CP and

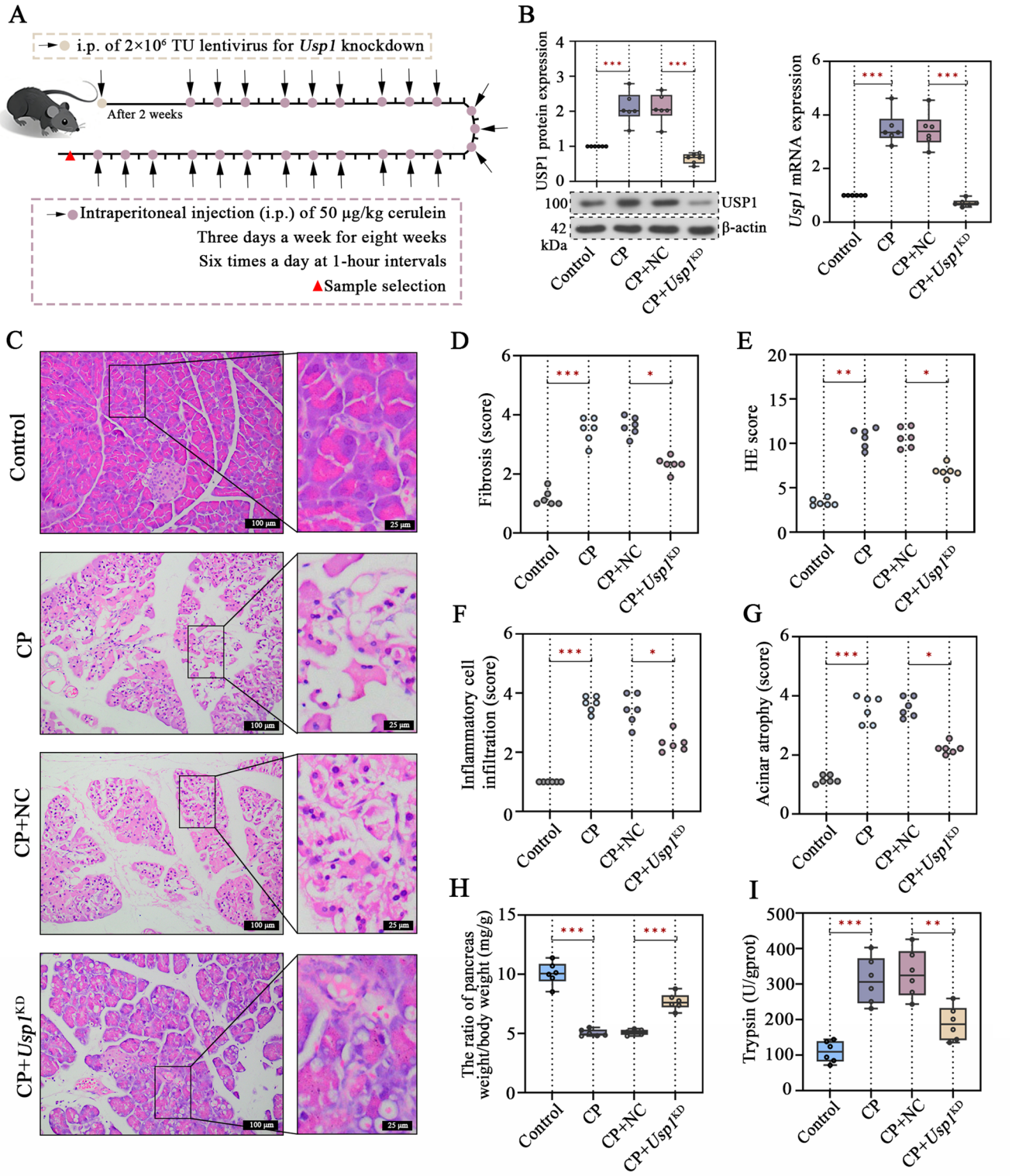

Fig. 2 *Usp1* knockdown alleviates cerubin-induced pancreatic tissue injury. (**A**) Flow chart of animal treatments. (**B**) USP1 expression in pancreatic tissues of cerulein-induced mice was detected by real-time PCR and western blot (n=6). **C**-**G**. **H&E** staining and pathological score ($n=6$). Bar: left, 100 μm; right, 25 μm. H. The ratio of pancreas weigh/body weight. I. The activity of trypsin in pancreas ($n=6$). **, $p<0.01$; ***, $p<0.001$

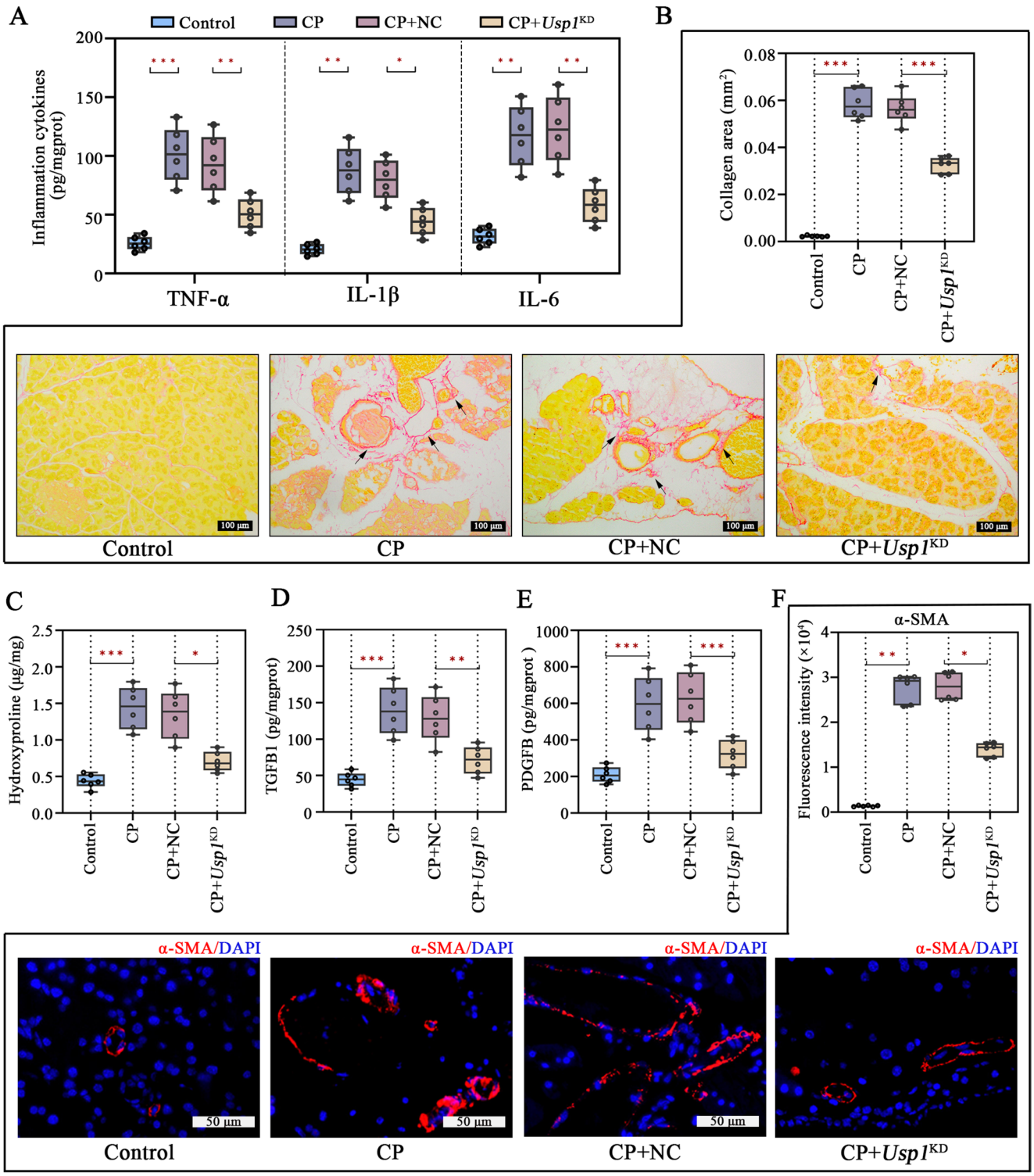

Fig. 3 *Usp1* knockdown alleviates fibrosis in pancreatic tissues of CP mice. (**A**) The levels of TNF-α, IL-1β, and IL-6 in pancreatic tissues were detected by ELISA ($n=6$). (**B**) Sirius red staining of mouse pancreatic tissues ($n=6$). Bar: 100 μm. Black arrows indicate areas of fiber deposition. (**C**) The Hydroxyproline content in pancreatic tissues was detected ($n=6$). **D-E**. The levels of TGFB1 (**D**) and PDGFB (**E**) in pancreatic tissues were measured by ELISA ($n=6$). **F**. Immunofluorescence staining of α-SMA in pancreatic tissues ($n=6$). Bar: 50 μm. **, $p<0.01$; ***, $p<0.001$

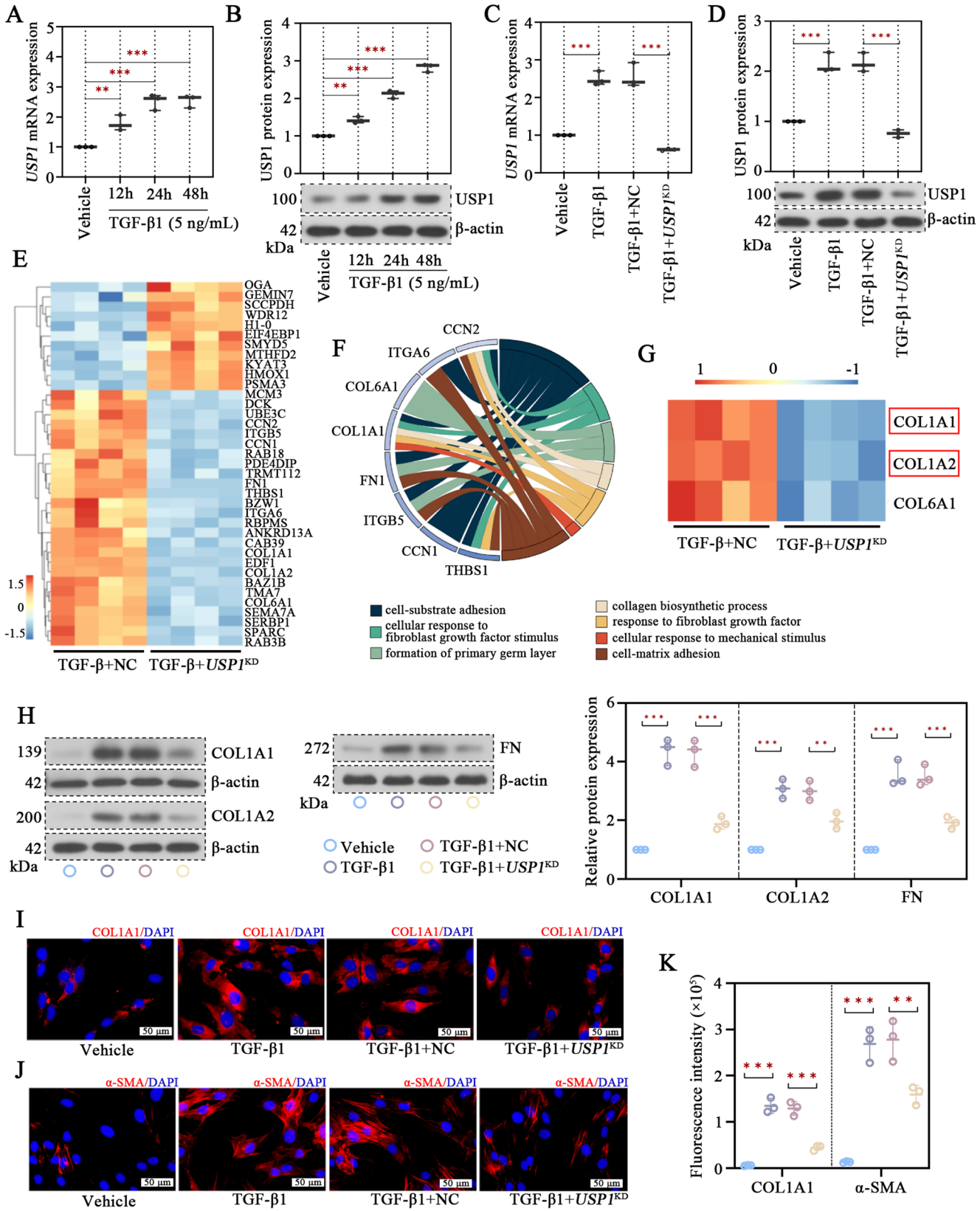
A
USP1 mRNA expression
Vehicle
12h 24h 48h
TGF-β1 (5 ng/mL)
B
USP1 protein expression
USP1
β-actin
kDa
C
USP1 mRNA expression
Vehicle
TGF-β1
TGF-β1+NC
TGF-β1+USP1KD
D
USP1 protein expression
E
OGA
GEMIN7
SCCPDH
WDR12
H1-0
EIF4EBP1
SMYD5
MTHFD2
KYAT3
HMOX1
PSMA3
MCM3
DCK
UBE3C
CCN2
ITGB5
CCN1
RAB18
PDE4DIP
TRMT112
FN1
THBS1
BZW1
ITGA6
RBPMS
ANKRD13A
CAB39
COL1A1
EDF1
COL1A2
BAZ1B
TMA7
COL6A1
SEMA7A
SERBP1
SPARC
RAB3B
TGF-β+NC
TGF-β+USP1KD
F
CCN2
ITGA6
COL6A1
COL1A1
FN1
ITGB5
CCN1
THBS1
cell-substrate adhesion
cellular response to fibroblast growth factor stimulus
formation of primary germ layer
collagen biosynthetic process
response to fibroblast growth factor
cellular response to mechanical stimulus
cell-matrix adhesion
G
COL1A1
COL1A2
COL6A1
TGF-β+NC
TGF-β+USP1KD
H
COL1A1
β-actin
COL1A2
FN
Vehicle
TGF-β1
TGF-β1+NC
TGF-β1+USP1KD
Relative protein expression
I
COL1A1/DAPI
50 μm
J
α-SMA/DAPI
K
Fluorescence intensity (×10⁵)
α-SMA

Fig. 4 Proteomics reveals impairment of ECM degradation in PSCs with *USP1* knockdown. **A**, **B**. USP1 expression was estimated in PSCs treated with different concentration of TGF-β1 (n = 3). **C**, **D**. The USP1 expression after lentiviral transfection was detected by real-time PCR (**C**) and western blot (**D**) ($n = 3$). E Heap map of differentially expressed proteins (DEPs) in label-free proteomic ($n = 4$). **F**. GO enrichment analysis of DEPs associated with collagen fibers. **G**. Heat map of collagen protein (n = 4). **H**. The protein expression of COL1A1, COL1A2, and FN in the PSCs was determined by western blot ($n = 3$). **I**. Immunofluorescence staining of COL1A1 in the PSCs ($n = 3$). Bar: 50 μm. **J**. Immunofluorescence staining of α-SMA. Bar: 50 μm. **K**. Quantitative analysis of the fluorescence intensity of COL1A1 (**I**) and α-SMA (J) ($n = 3$). **, $p < 0.01$; ***, $p < 0.001$

identify potential therapeutic targets [23–25]. While pancreatic weight may be affected by pancreatic edema in the early stage of acute pancreatitis, a decrease in pancreatic weight following chronic injury typically indicates pancreatic atrophy [26]. Consistently, in our study, one week after cerulein induction, pancreatic weight was significantly reduced, suggesting that pancreatic fibrosis and atrophy had developed.

CP typically evolves from repeated episodes of acute pancreatitis [27]. In the present study, a mouse model of CP was established via 8 weeks of cerulein induction. Chronic pancreatic inflammation triggers tissue fibrosis and atrophy [28, 29]. Following cerulein induction, pancreatic tissues exhibited fibrosis and atrophy with time-dependent pathological damage; these pathological manifestations confirmed the successful establishment of our mouse CP model. Notably, we analyzed the GSE41418 dataset and found that *Usp1* expression was significantly upregulated in pancreatic tissues of cerulein-induced mice. Consistent with this database result, our experimental data also demonstrated elevated USP1 expression in cerulein-induced mice. Collectively, we hypothesized that USP1 promotes pancreatic fibrosis and thereby drives CP progression by enhancing inflammation and activating PSCs.

The ubiquitin-proteasome system comprises an enzymatic cascade that regulates protein ubiquitination, which post-translationally modifies target proteins by covalently attaching one or more ubiquitin molecules to their lysine residues [30, 31]. USP1, a member of the ubiquitin-specific protease family, modulates protein stability via deubiquitination, thereby regulating cellular biological processes [6]. In the present study, USP1 expression in pancreatic tissues was knocked down using a constructed lentiviral vector. In pancreatitis, cholecystokinin stimulates pancreatic enzyme secretion, and excessive pancreatic enzyme release causes further digestive damage to pancreatic tissue, exacerbating pancreatic necrosis [32–34]. Interestingly, *Usp1* knockdown alleviated inflammatory infiltration in pancreatic tissues and reduced trypsin activity, which collectively inhibited CP progression. Furthermore, Sirius red staining showed that *Usp1* knockdown decreased the Sirius red-positive area, indicating that USP1 promotes pancreatic fibrosis.

PSCs account for only 4–7% of pancreatic cells [35], while they play a critical role in pancreatic diseases. In CP, PSCs transition from a quiescent to an activated state, acquiring a myofibroblast-like phenotype [36], and activated PSCs then contribute to collagen fiber deposition and drive pancreatic fibrosis progression [37]. TGF-β is a key mediator in the activation of PSCs, promoting their secretion of ECM components [38]. Label-free proteomics enables the construction of protein interaction networks and analysis of protein expression changes under different treatments. Our proteomic results showed that the expression of COL1A1 and COL1A2 was downregulated after *USP1* knockdown, and this finding was further validated by western blot analysis. Additionally, GO analysis revealed that DEPs following *USP1* knockdown were enriched in biological processes such as collagen biosynthetic process, fibroblast growth factor signaling, and cell-matrix adhesion—results that further confirm USP1's role in regulating ECM metabolism in PSCs. Notably, abnormally activated pancreatic enzymes cause pancreatic tissue damage and further stimulate PSC activation [39]. α-SMA is widely recognized as a marker of PSC activation [40, 41] and α-SMA-positive cells are detectable in disease-associated fibroblasts from patients with pancreatic cancer and CP [42]. Furthermore, a previous study reported elevated α-SMA expression in cerulein-induced mice [43]. Consistently, our study showed that α-SMA expression in pancreatic tissues was increased after 8 weeks of cerulein induction, indicating PSC activation, whereas *Usp1* knockdown suppressed this activation. It has been reported that TGF-β1 and PDGFB mediate PSC activation by transcriptionally regulating α-SMA and COL1A1 [3, 44]. We therefore examined the expression of TGF-β1 and PDGFB in our model. As expected, both them were highly expressed in the pancreatic tissues of CP mice, and *Usp1* knockdown significantly inhibited their expression. Collectively, these findings demonstrate that *Usp1* knockdown suppresses PSC activation in CP.

To investigate the specific mechanism of USP1, we conducted IP-LC/MS and label-free proteomics to identify downstream targets of USP1. Cross-analysis revealed that ITGB5 was the only protein present at the intersection of the three datasets. The cytoplasmic domain tail of ITGB5 contains four lysine residues [12], which are potential ubiquitination sites. USP10, another member of the USP family, can inhibit ITGB5 ubiquitination [15].this inhibition maintains ITGB5 protein stability, thereby promoting the expression of α-SMA and FN [15]. Notably, a previous study demonstrated that ITGB5 enhances proliferation and migration in pancreatic adenocarcinoma [45], indicating its potential involvement in pancreatic-related diseases. In our study, *USP1* knockdown reduced ITGB5 protein expression in both CP mice and TGF-β-stimulated PSCs. Furthermore,

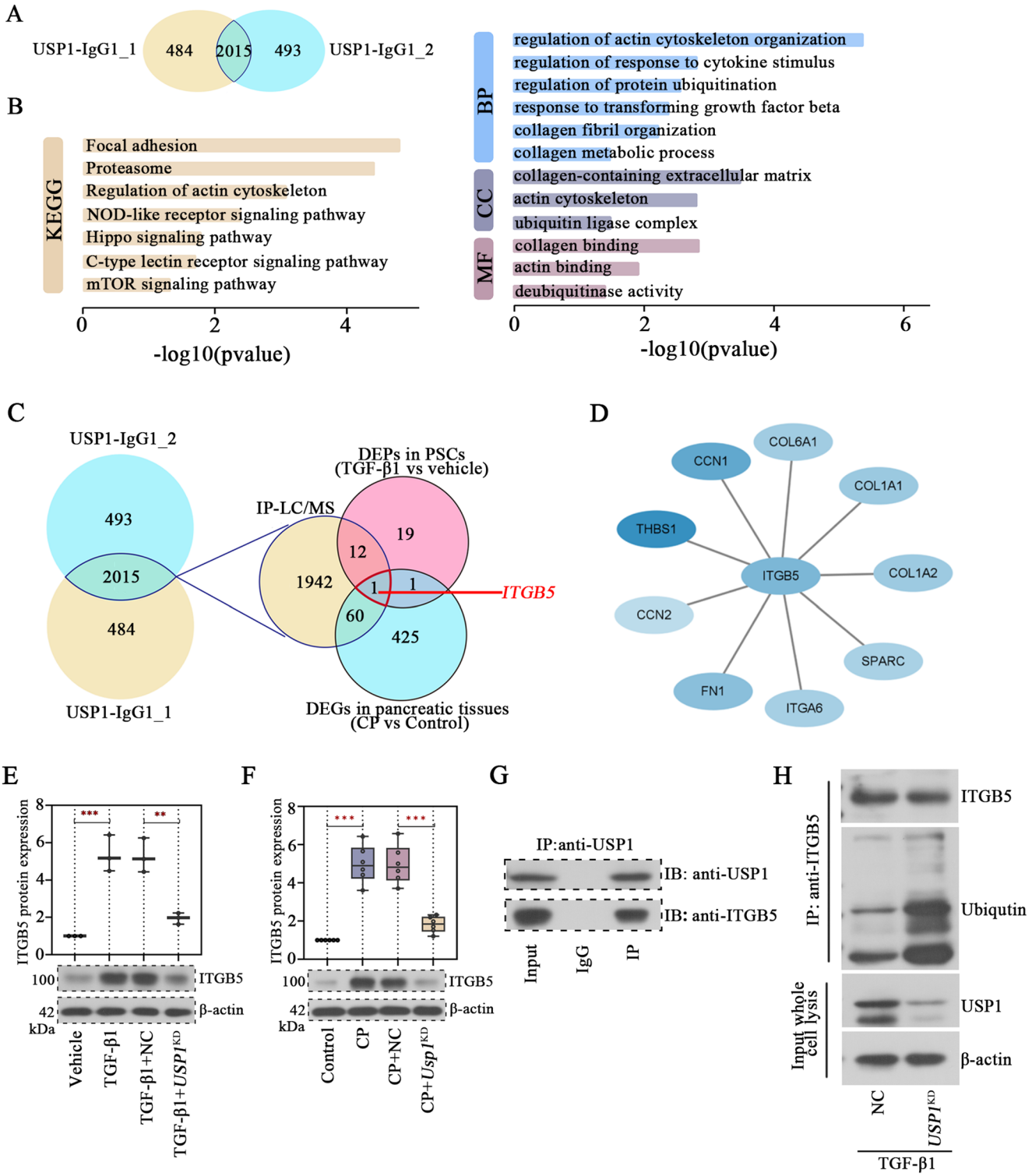

Fig. 5 *USP1* knockdown promotes ITGB5 ubiquitination-mediated degradation. (**A**) Venn plot showing a total of 2015 proteins bind to USP1 under TGF-β1 stimulation. (B) KEGG pathway analysis and GO enrichment analysis pair of 2015 proteins in (**A**). (**C**) Label-free proteomics combined with IP-LC/MS to analysis the USP1 downstream target. The intersection of differential downregulated expressed protein of label-free proteomics, IP-LC/MS, and the upregulated genes of GSE41418 dataset. (**D**) The ITGB5-associated PPI was established via the String database. E-F. The expression of ITGB5 of the PSCs (E) ($n=3$) and pancreatic tissues (**F**) ($n=6$) was estimated by western blot. **G**. Co-IP shows the interaction of USP1 and ITGB5 in the PSCs ($n=3$). **H**. Ubiquitination detection of ITGB5 in the PSCs were measured by Co-IP ($n=3$). **, $p<0.01$; ***, $p<0.001$.

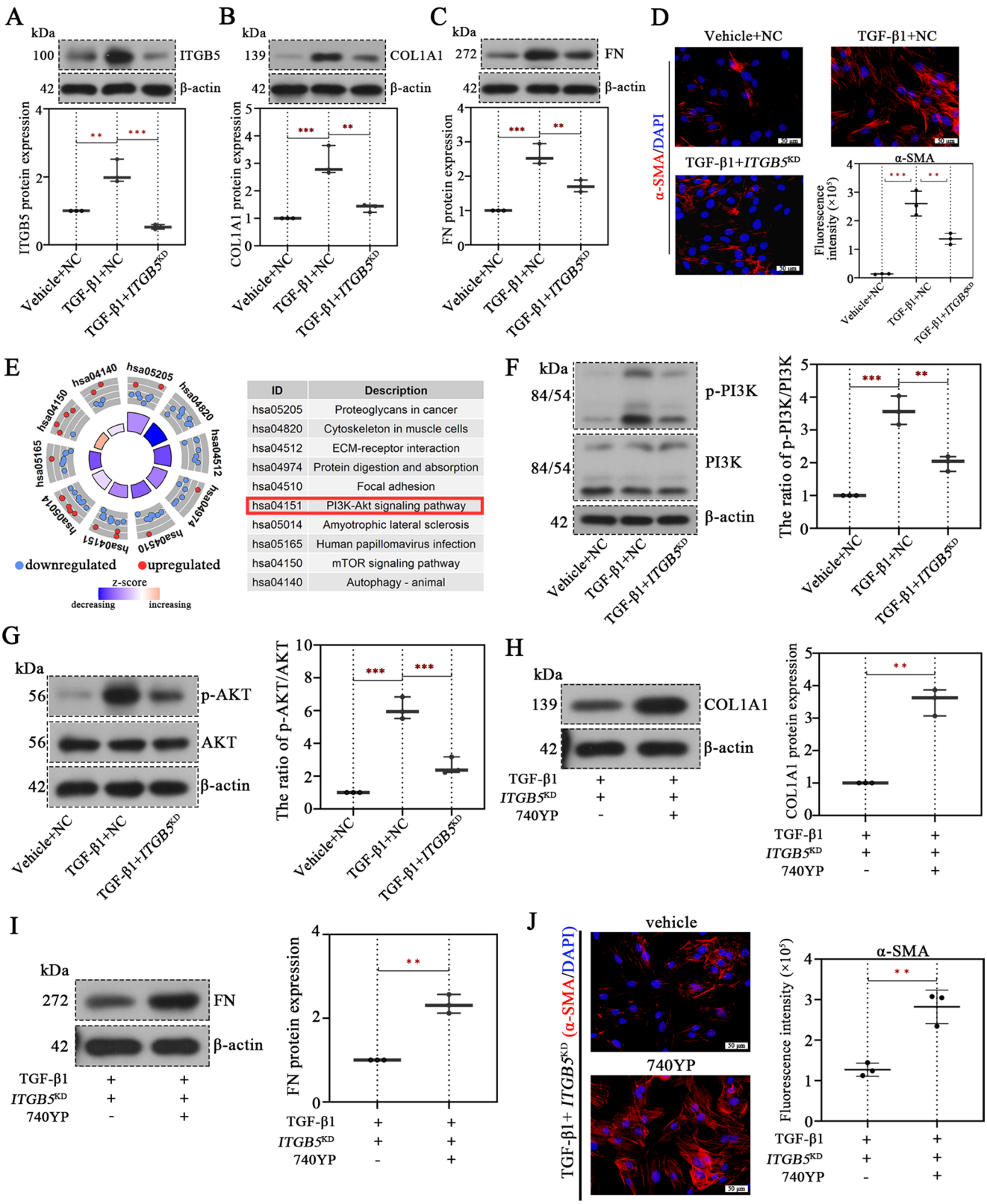

Fig. 6 *ITGB5* knockdown inhibits PSC activation by inhibiting the PI3K/AKT pathway. **A**. The ITGB5 expression in the PSCs after lentiviral transfection was detected by western blot (n=3). **B**, **C**. The expression of COL1A1 (**B**) and FN (**C**) was detected by western blot (n=3). **D**. IF staining showed the α-SMA expression (n=3). Bar: 50 μm. **E**. KEGG analysis of DEPs of label-free proteomics. **F**, **G**. The phosphorylation levels of PI3K and AKT and the PI3K and AKT protein expression was measured by western blot (n=3). **H**, **I**. The expression of COL1A1 and FN was detected by western blot (n=3). **J**. α-SMA expression in the PSCs was determined by IF staining (n=3). Bar: 50 μm. **, p<0.01; ***, p<0.001.

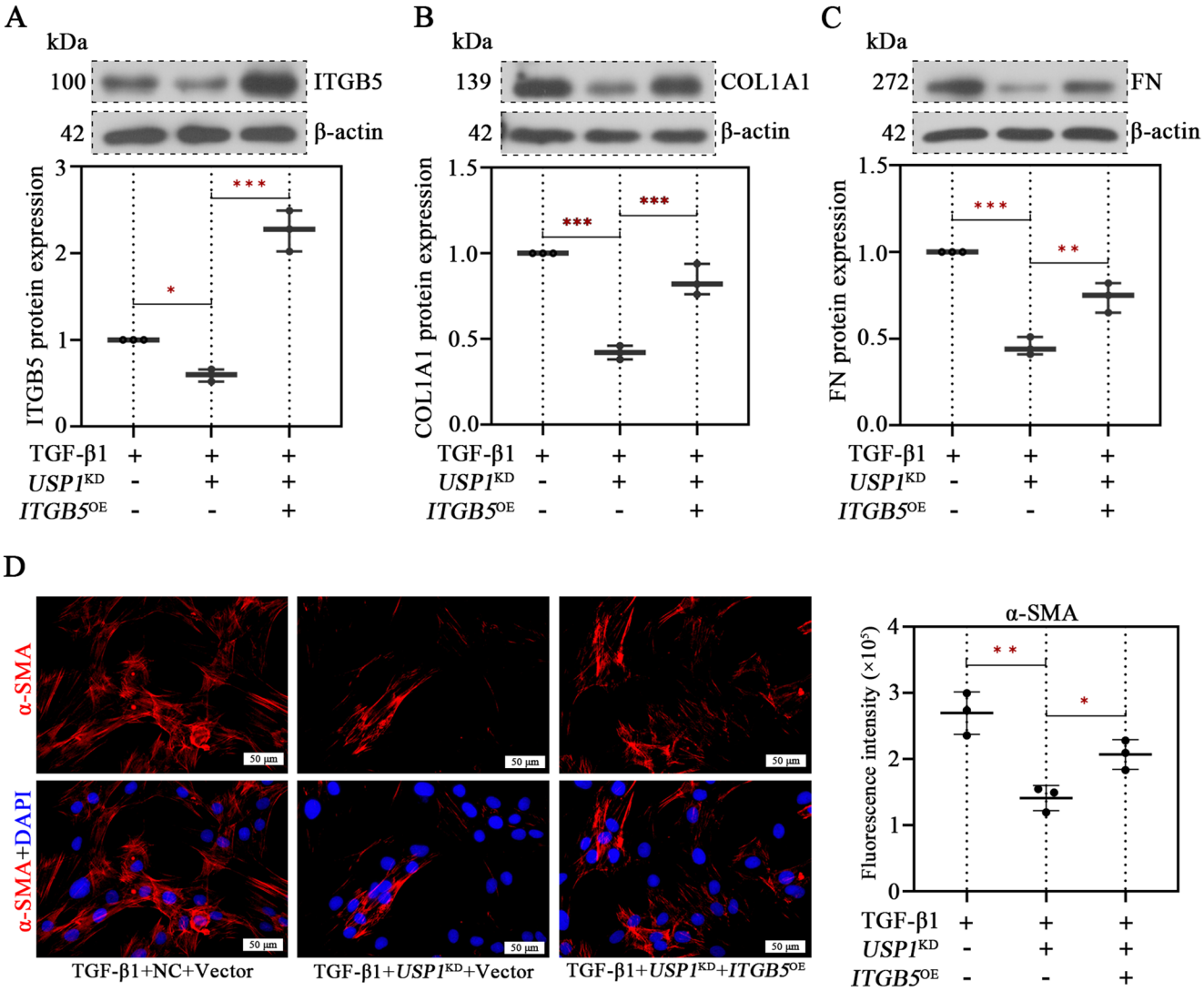

Fig. 7 *ITGB5* overexpression increased extracellular matrix. (**A**) ITGB5 expression in the PSCs was detected by western blot ($n=3$). (**B**) COL1A1 expression in the PSCs was detected by western blot ($n=3$). (C) FN expression in the PSCs was detected by western blot ($n=3$). (**D**) Immunofluorescence staining of α-SMA in the PSCs ($n=3$). Bar: 50 μm. *, $p<0.05$; **, $p<0.01$; ***, $p<0.001$.

Co-IP results showed that USP1 could interact with ITGB5. Importantly, *USP1* knockdown promoted ITGB5 ubiquitination and subsequent protein degradation. These findings demonstrate that USP1 enhances ITGB5 deubiquitination and stabilizes ITGB5 protein levels. The role of ITGB5 in the fibrotic process has been reported [15]. Additionally, activation of the PI3K/AKT pathway is known to promote PSC activation [46, 47]. Our proteomic results showed that DEPs in *USP1*-knockdown samples were enriched in the PI3K/AKT pathway. Given that TGF-β1 activates the PI3K/AKT pathway in PSCs, we further investigated whether ITGB5, as a downstream target of USP1, regulates this pathway. Results showed that *ITGB5* knockdown inhibited PI3K/AKT activation, while treatment with 740 YP (a PI3K agonist) reversed the inhibitory effect of *ITGB5* knockdown on PSC activation. These data indicate that *ITGB5* knockdown suppresses PSC activation and fibrosis by inhibiting the PI3K/AKT pathway. Importantly, *USP1* knockdown inhibited the activation of PSCs, whereas *ITGB5* overexpression reversed this inhibitory effect.

At present, USP1 inhibitors are mainly used to inhibit cancer progression [48, 49]. Other USP1 inhibitors, including SIM0501, XL309-101, and HSK39775, are currently in early clinical development [50]. Perhaps USP1 inhibitors also have the potential to alleviate non-neoplastic diseases, such as chronic pancreatitis. Future research should focus on developing pancreatic tissue-specific delivery systems. Specifically, nanoparticle carriers conjugated with pancreatic stellate cell-targeting ligands [51] can be utilized to improve the local accumulation of USP1/ITGB5 inhibitors while minimizing systemic toxicity. In addition, USP1 inhibitors in combination with existing antifibrotic drugs or

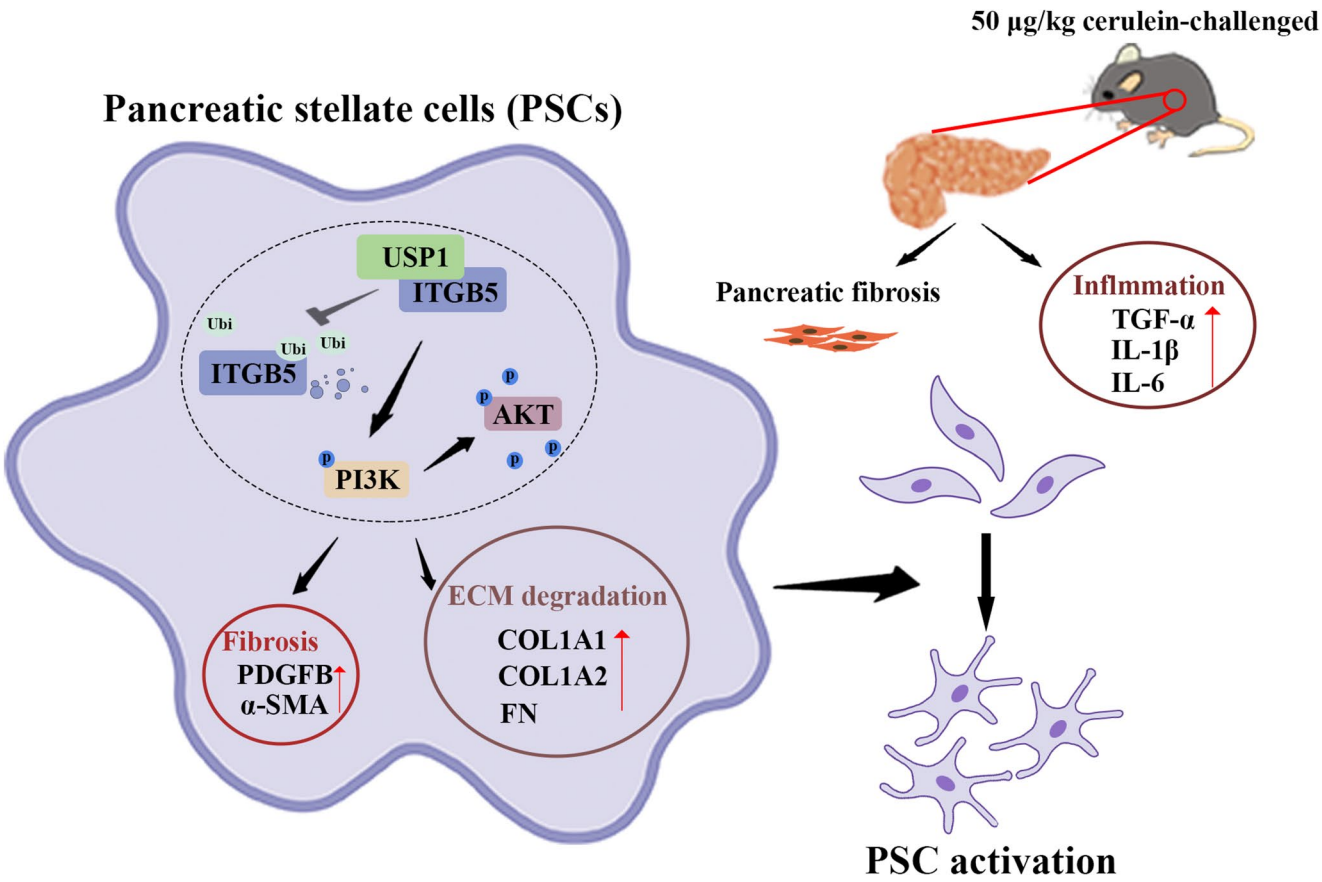

Fig. 8 Graphical summary of the possible mechanisms of USP1/ITGB5 axis in CP progression. USP1 deubiquitinates and stabilizes ITGB5, upregulates ITGB5 expression, and ITGB5 activated the PI3K/AKT pathway and subsequently activates PSCs, leading to pancreatic fibrotic injury in CP. Arrow: promotion; "tee" head: inhibition

anti-inflammatory drugs may synergistically inhibit PSC activation and alleviate established fibrosis, which is particularly important for treating patients with advanced CP with pancreatic damage.

Conclusions

Overall, our study (Fig. 8) demonstrated that USP1 deubiquitinates and stabilizes ITGB5, upregulates ITGB5 expression, and ITGB5 activated the PI3K/AKT pathway and subsequently activates PSCs, leading to pancreatic fibrotic injury in CP. developing drugs targeting the USP1-ITGB5-PI3K/AKT axis may provide a potential therapeutic strategy for preventing and mitigating pancreatic injury caused by CP.

Abbreviations

ANOVA	analysis of variance
cDNA	complementary DNA
Co-IP	Co-immunoprecipitation
COL1A1	collagen type I alpha 1 chain
CP	chronic pancreatitis
DAPI	dihydrochloride
DEGs	differentially expressed genes
DEPs	differentially expressed proteins
ECM	extracellular matrix
FN	fibronectin
FN-EDA	fibronectin extra domain A
GO	Gene Ontology
GSEA	Gene Set Enrichment Analysis
H&E	hematoxylin-eosin
IL-1β	interleukin-1β
IL-6	interleukin-6
IP-LC/MS	immunoprecipitation-liquid chromatography/mass spectrometry
ITGB5	integrin subunit beta 5
KEGG	Kyoto Encyclopedia of Genes and Genomes
NCBI	National Center for Biotechnology Information
NLRP3	nucleotide-binding oligomerization domain-like receptor pyrin domain-containing 3
PDGFB	platelet-derived growth factor subunit B
PPI	protein-protein interaction
PSCs	pancreatic stellate cells

PVDF	polyvinylidene fluoride
SD	standard deviation
SDS–PAGE	sodium dodecyl sulfate–polyacrylamide gel electrophoresis
TGF-β1	transforming growth factor-β1
TNF-α	tumor necrosis factor-α
USP1	ubiquitin-specific peptidase 1
α-SMA	α-smooth muscle actin

Supplementary Information The online version contains supplementary material available at https://doi.org/10.1007/s10753-025-02434-x.

Author Contributions Conceptualization: D.W., Y.S., and C.Z.; Methodology: D.W. and Y.S.; Formal analysis: J.L., W.B., and N.W.; Investigation: Q.S., Z.L., and L.Q.; Writing - original draft preparation: D.W. and Y.S.; Writing - review and editing: All authors; Supervision: C.Z.

Funding This study was supported by the "Three Navigation" Plan of Talent Training in Pudong New Area Gongli Hospital (2025-GLSHQH-03) to Dongyan Wang, Shanghai Municipal Health Commission Clinical Research Special Project of the Health Industry in 2025 (20254Y0066) to Dongyan Wang, the Investigator-initiated Trial Program of Shanghai Pudong New Area Health Commission (the Medical and Industrial Integration Program) (2025-PWYC-04) to Yihai Shi, Zhejiang Traditional Chinese Medicine Science and Technology Plan in 2025 (Young Talents Support Program Project) (NO. 2025ZR14) to Chang Zhu, National Natural Science Foundation of China (82370580) to Jie Lu, and Specialty Feature Construction Project of Pudong Health and Family Planning Commission of Shanghai（PWZzb2022-14) to Jie Lu..

Data Availability The datasets generated and/or analyzed during the current study are available from the corresponding author on reasonable request. The dataset GSE41418 can be obtained from the GEO database (https://www.ncbi.nlm.nih.gov/geo/query/acc.cgi?acc=GSE41418).

Declarations

Ethics Approval The study was approved by the ethics committee of Sir Run Run Shaw Hospital (No. SRRSH202402287).

Competing interests The authors declare no competing interests.

Clinical Trial Number Not applicable.

References

1. Witt, H., M. V. Apte, V. Keim, and J. S. Wilson. 2007. Chronic pancreatitis: Challenges and advances in pathogenesis, genetics, diagnosis, and therapy. *Gastroenterology* 132(4):1557–1573. https://doi.org/10.1053/j.gastro.2007.03.001
2. Nair, R. J., L. Lawler, and M. R. Miller. 2007. Chronic pancreatitis. *Am Fam Physician* 76(11):1679–1688.
3. Omary, M. B., A. Lugea, A. W. Lowe, and S. J. Pandol. 2007. The pancreatic stellate cell: A star on the rise in pancreatic diseases. *J Clin Invest* 117(1):50–59. https://doi.org/10.1172/JCI30082
4. Schmidt, M., and D. Finley. 2014. Regulation of proteasome activity in health and disease. *Biochimica Et Biophysica Acta* 1843(1):13–25. https://doi.org/10.1016/j.bbamcr.2013.08.012
5. Nandi, D., P. Tahiliani, A. Kumar, and D. Chandu. 2006. The ubiquitin-proteasome system. *Journal of Biosciences* 31(1):137–155. https://doi.org/10.1007/BF02705243
6. Garcia-Santisteban, I., G. J. Peters, E. Giovannetti, and J. A. Rodriguez. 2013. USP1 deubiquitinase: Cellular functions, regulatory mechanisms and emerging potential as target in cancer therapy. *Molecular Cancer* 12:91. https://doi.org/10.1186/1476-4598-12-91
7. Gorrepati, K. D. D., B. Lupse, K. Annamalai, T. Yuan, K. Maedler, and A. Ardestani. 2018. Loss of deubiquitinase USP1 blocks pancreatic beta-Cell apoptosis by inhibiting DNA damage response. *iScience* 1:72–86. https://doi.org/10.1016/j.isci.2018.02.003
8. Francis, M., S. Bhaskar, S. Komanduri, P. Sheshadri, J. Prasanna, and A. Kumar. 2023. Deubiquitinase USP1 influences the dedifferentiation of mouse pancreatic beta-cells. *iScience* 26(5):106771. https://doi.org/10.1016/j.isci.2023.106771
9. Li, J. T., K. Y. Li, Y. Su, Y. Shen, M. Z. Lei, and F. Zhang et al. 2022. Diet high in branched-chain amino acid promotes PDAC development by USP1-mediated BCAT2 stabilization. *Natl Sci Rev* 9(5):nwab212. https://doi.org/10.1093/nsr/nwab212
10. Song, H., C. Zhao, Z. Yu, Q. Li, R. Yan, and Y. Qin et al. 2020. UAF1 deubiquitinase complexes facilitate NLRP3 inflammasome activation by promoting NLRP3 expression. *Nature Communications* 11(1):6042. https://doi.org/10.1038/s41467-020-19939-8
11. Du, Z., T. Wu, L. Liu, B. Luo, and C. Wei. 2022. Ubiquitin specific peptidase 1 promotes hepatic fibrosis through positive regulation of CXCL1 by deubiquitinating SNAIL. *Digestive and Liver Disease : official Journal of the Italian Society of Gastroenterology and the Italian Association for the Study of the Liver* 54(1):91–102. https://doi.org/10.1016/j.dld.2021.02.025
12. Pasqualini, R., and M. E. Hemler. 1994. Contrasting roles for integrin beta 1 and beta 5 cytoplasmic domains in subcellular localization, cell proliferation, and cell migration. *Journal of Cell Biology* 125(2):447–460. https://doi.org/10.1083/jcb.125.2.447
13. Wang, L., B. S. Pedroja, E. E. Meyers, A. L. Garcia, S. S. Twining, and A. M. Bernstein. 2012. Degradation of internalized alphavbeta5 integrin is controlled by uPAR bound uPA: Effect on beta1 integrin activity and alpha-SMA stress fiber assembly. *PLoS One* 7(3):e33915. https://doi.org/10.1371/journal.pone.0033915
14. Lobert, V. H., A. Brech, N. M. Pedersen, J. Wesche, A. Oppelt, and L. Malerod et al. 2010. Ubiquitination of alpha 5 beta 1 integrin controls fibroblast migration through lysosomal degradation of fibronectin-integrin complexes. *Developmental Cell* 19(1):148–159. https://doi.org/10.1016/j.devcel.2010.06.010
15. Gillespie, S. R., L. J. Tedesco, L. Wang, and A. M. Bernstein. 2017. The deubiquitylase USP10 regulates integrin beta1 and beta5 and fibrotic wound healing. *Journal of Cell Science* 130(20):3481–3495. https://doi.org/10.1242/jcs.204628

16. Miyamoto, T., H. Nakamura, Y. Nagashio, H. Asaumi, M. Harada, and M. Otsuki. 2010. Overexpression of Smad6 exacerbates pancreatic fibrosis in murine caerulein-induced chronic pancreatic injuries. *Pancreas* 39(3):385–391. https://doi.org/10.1097/MPA.0b013e3181bb9603
17. Neuhöfer, P., S. Liang, H. Einwächter, C. Schwerdtfeger, T. Wartmann, and M. Treiber et al. 2012. Deletion of IκBα activates rela to reduce acute pancreatitis in mice through up-regulation of Spi2A. *Gastroenterology* 144(1):192–201. https://doi.org/10.1053/j.gastro.2012.09.058
18. Mao, X., S. Mao, L. Wang, H. Jiang, S. Deng, and Y. Wang et al. 2022. Single-Cell transcriptomic analysis of the mouse pancreas: Characteristic features of pancreatic ductal cells in chronic pancreatitis. *Genes (Basel)* 13(6). https://doi.org/10.3390/genes13061015
19. Inman, K. S., Y. Liu, M. L. Scotti Buzhardt, M. Leitges, M. Krishna, and H. C. Crawford et al. 2022. Prkci regulates autophagy and pancreatic tumorigenesis in mice. *Cancers (Basel)* 14(3):796. https://doi.org/10.3390/cancers14030796
20. Bombardelli, L., E. S. Carpenter, A. P. Wu, N. Alston, K. E. DelGiorno, and H. C. Crawford. 2010. Pancreas-specific ablation of beta1 integrin induces tissue degeneration by disrupting acinar cell Polarity. *Gastroenterology* 138(7):2531–2540. https://doi.org/10.1053/j.gastro.2010.02.043
21. Halbrook, C. J., H. J. Wen, J. M. Ruggeri, K. K. Takeuchi, Y. Zhang, and M. P. di Magliano et al. 2017. Mitogen-activated protein kinase kinase activity maintains Acinar-to-Ductal metaplasia and is required for organ regeneration in pancreatitis. *Cell Mol Gastroenterol Hepatol* 3(1):99–118. https://doi.org/10.1016/j.jcmgh.2016.09.009
22. Obafemi, T. F., P. Yu, J. Li, J. M. Davis, K. Liu, and B. Cheng et al. 2018. Comparable responses in male and female mice to Cerulein-Induced chronic pancreatic injury and recovery. *JOP* 19(5):236–243.
23. Neuschwander-Tetri, B. A., K. R. Bridle, L. D. Wells, M. Marcu, and G. A. Ramm. 2000. Repetitive acute pancreatic injury in the mouse induces Procollagen alpha1(I) expression colocalized to pancreatic stellate cells. *Laboratory Investigation* 80(2):143–150. https://doi.org/10.1038/labinvest.3780018
24. Aghdassi, A. A., J. Mayerle, S. Christochowitz, F. U. Weiss, M. Sendler, and M. M. Lerch. 2011. Animal models for investigating chronic pancreatitis. *Fibrogenesis Tissue Repair* 4(1):26. https://doi.org/10.1186/1755-1536-4-26
25. Ulmasov, B., K. Oshima, M. G. Rodriguez, R. D. Cox, and B. A. Neuschwander-Tetri. 2013. Differences in the degree of caerulein-induced chronic pancreatitis in C57BL/6 mouse substrains lead to new insights in identification of potential risk factors in the development of chronic pancreatitis. *American Journal of Pathology* 183(3):692–708. https://doi.org/10.1016/j.ajpath.2013.05.020
26. Geisz, A., and M. Sahin-Tóth. 2018. A preclinical model of chronic pancreatitis driven by trypsinogen autoactivation. *Nature Communications* 9(1):5033. https://doi.org/10.1038/s41467-018-07347-y
27. Singh, V. K., D. C. Whitcomb, P. A. Banks, S. AlKaade, M. A. Anderson, and S. T. Amann et al. 2022. Acute pancreatitis precedes chronic pancreatitis in the majority of patients: Results from the NAPS2 consortium. *Pancreatology* 22(8):1091–1098. https://doi.org/10.1016/j.pan.2022.10.004
28. DiMagno, E. P. 1993. A short, eclectic history of exocrine pancreatic insufficiency and chronic pancreatitis. *Gastroenterology* 104(5):1255–1262. https://doi.org/10.1016/0016-5085(93)90332-7
29. Ewald, N., and P. D. Hardt. 2013. Diagnosis and treatment of diabetes mellitus in chronic pancreatitis. *World Journal of Gastroenterology* 19(42):7276–7281. https://doi.org/10.3748/wjg.v19.i42.7276
30. Peng, J., W. Li, B. Wang, S. Zhang, Y. Xiao, and F. Han et al. 2022. UBE2G1 is a critical component of immune response to the infection of Pseudomonas plecoglossicida in large yellow croaker (Larimichthys crocea). *International Journal of Molecular Sciences* 23(15):8298. https://doi.org/10.3390/ijms23158298
31. Sun, T., Z. Liu, F. Bi, and Q. Yang. 2021. Deubiquitinase PSMD14 promotes ovarian cancer progression by decreasing enzymatic activity of PKM2. *Molecular Oncology* 15(12):3639–3658. https://doi.org/10.1002/1878-0261.13076
32. Sah, R. P., R. K. Dawra, and A. K. Saluja. 2013. New insights into the pathogenesis of pancreatitis. *Current Opinion in Gastroenterology* 29(5):523–530. https://doi.org/10.1097/MOG.0b013e328363e399
33. Boonchan, M., H. Arimochi, K. Otsuka, T. Kobayashi, H. Uehara, and T. Jaroonwitchawan et al. 2021. Necroptosis protects against exacerbation of acute pancreatitis. *Cell Death and Disease* 12(6):601. https://doi.org/10.1038/s41419-021-03847-w
34. Han, L., Z. Zhao, X. Chen, K. Yang, Z. Tan, and Z. Huang et al. 2022. Human umbilical cord mesenchymal stem cells-derived exosomes for treating traumatic pancreatitis in rats. *Stem Cell Research & Therapy* 13(1):221. https://doi.org/10.1186/s13287-022-02893-1
35. Ferdek, P. E., and M. A. Jakubowska. 2017. Biology of pancreatic stellate cells-more than just pancreatic cancer. *Pflugers Archiv. European Journal of Physiology* 469(9):1039–1050. https://doi.org/10.1007/s00424-017-1968-0
36. Cabrera, M. C., E. Tilahun, R. Nakles, E. S. Diaz-Cruz, A. Charabaty, and S. Suy et al. 2014. Human pancreatic Cancer-Associated stellate cells remain activated after in vivo chemoradiation. *Frontiers in Oncology* 4:102. https://doi.org/10.3389/fonc.2014.00102
37. Wang, Z., S. Dong, and W. Zhou. 2024. Pancreatic stellate cells: Key players in pancreatic health and diseases (Review). *Molecular Medicine Reports* 30(1). https://doi.org/10.3892/mmr.2024.13233
38. Sarper, M., E. Cortes, and T. J. Lieberthal. 2016. Del Río Hernández A. ATRA modulates mechanical activation of TGF-β by pancreatic stellate cells. *Scientific Reports* 6:27639. https://doi.org/10.1038/srep27639
39. Yao, W., D. Luo, Z. Lv, Y. Yang, L. Wang, and B. Ma et al. 2022. The Rabep1-Mediated endocytosis and activation of trypsinogen to promote pancreatic stellate cell activation. *Biomolecules* 12(8):1063. https://doi.org/10.3390/biom12081063
40. Ulmasov, B., B. A. Neuschwander-Tetri, J. Lai, V. Monastyrskiy, T. Bhat, and M. P. Yates et al. 2016. Inhibitors of Arg-Gly-Asp-Binding integrins reduce development of pancreatic fibrosis in mice. *Cell Mol Gastroenterol Hepatol* 2(4):499–518. https://doi.org/10.1016/j.jcmgh.2016.03.004
41. Lerch, M. M., and F. S. Gorelick. 2013. Models of acute and chronic pancreatitis. *Gastroenterology* 144(6):1180–1193. https://doi.org/10.1053/j.gastro.2012.12.043
42. Sunami, Y., Y. Chen, B. Trojanowicz, M. Sommerer, M. Hammerle, and R. Eils et al. 2022. Single cell analysis of cultivated fibroblasts from chronic pancreatitis and pancreatic cancer patients. *Cells* 11(16):2583. https://doi.org/10.3390/cells11162583
43. Sendler, M., G. Beyer, U. M. Mahajan, V. Kauschke, S. Maertin, and C. Schurmann et al. 2015. Complement Component 5 Mediates Development of Fibrosis, via Activation of Stellate Cells, in 2 Mouse Models of Chronic Pancreatitis. Gastroenterology. ;149(3):765–76 e10; https://doi.org/10.1053/j.gastro.2015.05.012
44. Kordes, C., S. Brookmann, D. Haussinger, and H. Klonowski-Stumpe. 2005. Differential and synergistic effects of platelet-derived growth factor-BB and transforming growth factor-beta1 on activated pancreatic stellate cells. *Pancreas* 31(2):156–167. https://doi.org/10.1097/01.mpa.0000168222.05591.a0

45. Wen, X., S. Chen, X. Chen, H. Qiu, W. Wang, and N. Zhang et al. 2022. ITGB5 promotes innate radiation resistance in pancreatic adenocarcinoma by promoting DNA damage repair and the MEK/ERK signaling pathway. *Frontiers in Oncology* 12:887068. https://doi.org/10.3389/fonc.2022.887068
46. Masamune, A., and T. Shimosegawa. 2009. Signal transduction in pancreatic stellate cells. *Journal of Gastroenterology* 44(4):249–260. https://doi.org/10.1007/s00535-009-0013-2
47. Estaras, M., R. Martinez, A. Garcia, C. Ortiz-Placin, J. L. Iovanna, and P. Santofimia-Castano et al. 2022. Melatonin modulates metabolic adaptation of pancreatic stellate cells subjected to hypoxia. *Biochemical Pharmacology* 202:115118. https://doi.org/10.1016/j.bcp.2022.115118
48. Wu, L., M. Yu, H. Liang, L. Lin, H. Li, and G. Chen et al. 2025. SJB2-043, a USP1 Inhibitor, suppresses A549 cell Proliferation, Migration, and EMT via modulation of PI3K/AKT/mTOR, MAPK, and Wnt signaling pathways. *Current Issues in Molecular Biology* 47(3). https://doi.org/10.3390/cimb47030155
49. Wang, L., T. Hu, Z. Shen, Y. Zheng, Q. Geng, and L. Li et al. 2022. Inhibition of USP1 activates ER stress through Ubi-protein aggregation to induce autophagy and apoptosis in HCC. *Cell Death & Disease* 13(11):951. https://doi.org/10.1038/s41419-022-05341-3
50. Torrado, C., N. W. Ashton, A. D. D'Andrea, and T. A. Yap. 2025. USP1 inhibition: A journey from target discovery to clinical translation. *Pharmacology & Therapeutics* 271:108865. https://doi.org/10.1016/j.pharmthera.2025.108865
51. Elechalawar, C. K., M. N. Hossen, P. Shankarappa, C. J. Peer, W. D. Figg, and J. D. Robertson et al. 2020. Targeting pancreatic cancer cells and stellate cells using designer nanotherapeutics in vitro. *Int J Nanomedicine* 15. https://doi.org/10.2147/IJN.S234112